

Drop Impact onto a Metallic Porous Layer: Scale Effects

Cristina Boscaroli¹, Dipak Sarker², Cyril Crua¹, Marco Marengo¹

¹School of Computing Engineering and Mathematics, University of Brighton, United Kingdom

²School of Pharmacy and Biomolecular Science, University of Brighton, United Kingdom

*Corresponding author: c.boscaroli@brighton.ac.uk

Abstract

The study of drop impact, spreading and rupture, has an obvious relevance in different fields. In this work the isothermal impact of drop on a metallic mesh is investigated. The outcome of a drop impact can be well predicted for smooth surfaces, but the effects of surface topology is not yet fully understood. The aim of this paper is investigating the outcome of a droplet impact onto a metallic mesh, which represents a specific porous layer with different pore dimensions. The experiments carried out in this study consisted of water drop of water impacting on stainless steel meshes with a mean pore size ranging from 25 to 425 μm and a thickness ranging from 25 to 125 μm . The meshes are lying on a flat solid surface made of stainless steel and their vertical movement is reduced as much as possible using a steel ring. A combination of surface with a different dimension of pores size and different liquids (water and acetone) is necessary to study their respective influence. The Range of Weber, Reynolds and Ohnesorge number is respectively between 100-1400, 2500-20000 and 0.0015-0.0032. It is found that by increasing the pore dimension, a faster imbibition occurs and, in this case, the spreading does not depend on the impact Weber number because, even if the impact occurs at a higher velocity, it is limited by the imbibition.

Introduction

The droplet impact on porous surfaces can be linked to different applications, such as distribution of agrochemicals, where droplets are distributed as aqueous solution and sprayed on plants by using pumps [1], the infiltration of rain and surface water into soil, the migration of oil in permeable porous media and the deposition of dyes on papers in the ink-jet printing process [2]. Porous surfaces find an application even considering internal combustion engines. In fact, a porous layer can be used in order to perform fuel vaporization and increase fuel distribution in space, obtaining a homogeneous and low emission combustion. The full applicability of this technique must still be experimentally verified [3]. Considering the sheer number of practical applications that involve surfaces of higher complexity like textured or porous surfaces, the number of parameters influencing droplet impact is vast. For this reason, a range of numerical and experimental investigations is still required, in order to quantify for example the imbibition due to porosity and identify the outcome of the impacts [4]. Roisman et al. [5] developed a model describing the different regimes of splashing thresholds by analysing two substrate characteristics: roughness and porosity. They proposed an experimental map obtained by different combinations of Reynolds, Weber numbers and surface roughnesses, concluding that the two most significant parameters influencing the prompt splash-position are the Weber number and the ratio given by two geometrical characteristics linked to roughness. They found more difficult to understand the experimental results on impact onto porous substrates due to irregular morphologies of the target, and the addition of several parameters to the problem, such as substrate porosity and pore diameter. They observed that in the case of porous surfaces, deposition without splash is more probable. This outcome may be due to a rapid, partial penetration of the drop into the target but further work is needed to clarify this phenomenon. Neyval et al. [6], developed a numerical model to analyse the impact of a droplet on a porous medium including the effect of surface of the medium. They compared their results with experimental data. The results showed good agreement with most of the data, except for a small deviation in the case of droplet impinging on an unconsolidated substrate (substrate whose particle are not cemented together) with very small particles, disrupted by the impact of the liquid, an effect that in particular was not considered in the code. Sahu et al. [7] studied the impact of nanoparticle suspension into porous filter membranes focusing on penetration given by the hydrodynamic effect, phenomenon caused by the kinetic energy brought by a drop, which impacts on porous media having a very small pore size with respect to drop size. They compared this aspect with the effect given by dynamic and capillary pressure and concluded that penetration into porous medium is possible when the dynamic pressure is higher than capillary pressure, but also when hydrodynamic focusing, that occurs when the drop diameter is much larger than pore diameter, is observed. Zouhaier et al. [8] analysed droplet impact on a textile material made by virgin glass, a dispersive coating solution obtained by a textile printing process, set down by spin-coating on the glass and woven cotton fabric at different construction parameters. They identified three different drop-spreading phases, finding that the droplet profile is influenced by fabric porosity compared to impacts on the virgin glass and coating film. Woo et

al. [9] analysed the thermal and hydrodynamic behaviour of a water drop impinging on heated porous surfaces observing that increasing the size of the sintered pores, spreading ratio and permeation time decreased. This research aims at defining a map of regimes to describe the different kind of outcomes given by drop impact, for different combinations of pore dimension, impact velocity, drop radius, liquid surface tension and viscosity. Pore dimension is defined as the mean pore diameter. In order to identify the different regions of the transition map, it was chosen to make reference to the dynamic (p_d) and capillary (p_c) pressures

$$p_d = \frac{1}{2} \rho v_i^2 \quad p_c = \frac{\sigma}{D_{pore}} \quad (1)$$

where ρ is the density of the droplet, v_i the impact velocity, σ the surface tension and D_{pore} the mean pore diameter. The flow characteristics are mainly described thanks to the dimensionless Weber and Reynolds number [10]

$$We = \frac{\rho d v_i^2}{\sigma} \quad Re = \frac{\rho d v_i}{\mu} \quad (2)$$

where d is the droplet diameter and μ the liquid viscosity.

In defining a dimensionless number given by the ratio between pore diameter and drop diameter, $\frac{D_{pore}}{d}$. In clarifying the roles that the dimensionless diameter has on the impact outcome, without avoiding the effects of impact velocity and liquid characteristics, a more thorough prediction of drop impact outcome on complex surface could be achievable.

By reporting a transition map with respect to $\frac{p_c}{p_d}$ and the Weber number, the experiments are aimed at outlining the different drop impact regimes. At lower values of impact velocity ($p_c > p_d$) deposition occurs, otherwise, increasing the value of impact velocity ($p_d > p_c$) an imbibition is obtained. Kumar et al. [11] pointed out that the overall imbibition is influenced both by the material of the porous media and capillary and showed that increasing drop size brings to a slower imbibition. The third region describes the splashing threshold, reached by a further increase of impact velocity. The general trends of impact outcomes given by the present work are shown in the video sequences below.

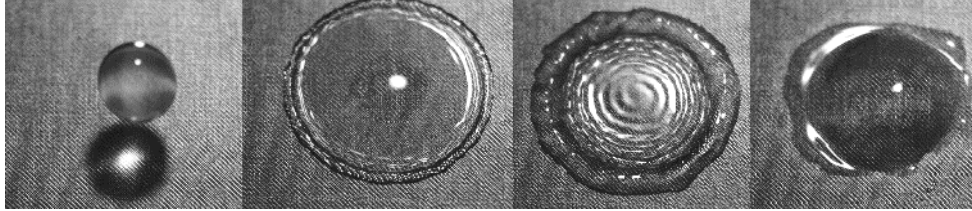


Figure 1. Deposition outcome: $d = 3,019 \text{ mm}$, $v_i = 1,76 \text{ m/s}$, $D_{pore} = 25 \mu\text{m}$

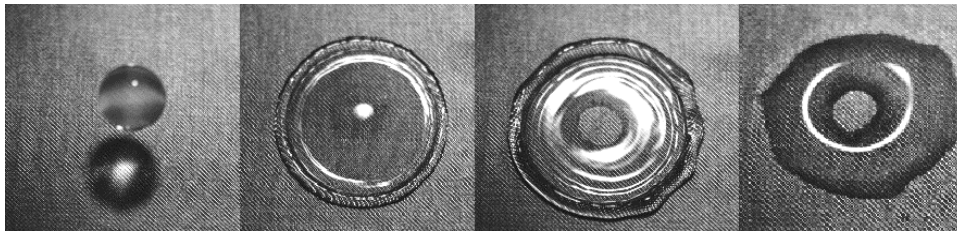


Figure 2. Partial imbibition outcome: $d = 3,065 \text{ mm}$, $v_i = 1,71 \text{ m/s}$, $D_{pore} = 25 \mu\text{m}$ → Same impact parameters, different outcome.

The first results obtained show clearly that a more accurate description of what happen in the transition region between deposition and imbibition has to be given. In fact, in the specific case, even without changing any parameter of the set-up (same height of release and same needle), different outcomes are observed.

Material and methods

The experiments carried out in this study consisted of single water, dodecane or acetone drops impacting on stainless steel meshes, mainly used for filtration applications, purchased from Plastock (COUNTRY), with a mean pore size ranging from 25 to 425 μm and a thickness ranging from 25 to 125 μm . A combination of different surface porosities and liquids is needed in order to study how the impact outcome is influenced; Conversely it is also necessary to use the same materials for the sample in order to observe the effect due to porosity without changing other properties like wettability. In order to avoid elasticity due to the thin thickness of the meshes, it was necessary

to carefully attach the meshes to a flat surface, pressed by means of a steel ring (see Figure 4). In order to have meaningful consistent data and to evaluate the repeatability of the experimental results, each impact case was performed and recorded at least 10 times. The optical setup included a Photron Fastcam SA4 high speed camera (with a resolution of 1024x800 pixels), and angled at 61° with respect to the horizontal plane. The test area was illuminated using a custom-built high-speed LED light source, synchronised to the high-speed camera.

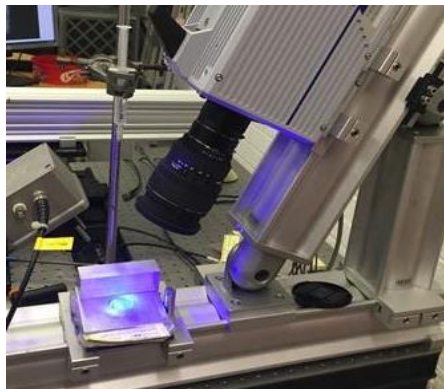


Figure 3 Optical Set-up

The drops were generated using needles of two different sizes: a 21 gauge needle, with inner diameter 514 μm and outer diameter 819 μm and a 26s gauge needle, with inner diameter of 173.4 μm and outer diameter of 473.7 μm . In order to change impact velocity, the system is designed to release droplets manually from three different heights, to obtain a range of velocities between 1.5 and 4.0 m/s. In the following tables the characteristics of the mesh and the liquid used for the experiments are reported.

Table 1 Mesh material and pores dimension.

Sample Number	Mesh Material	Pore Diameter (μm)	Wire Diameter (μm)
1	Stainless Steel	25	0.025
2	Stainless Steel	50	0.036
3	Stainless Steel	80	0.05
4	Stainless Steel	100	0.065
5	Stainless Steel	125	0.1
6	Stainless Steel	150	0.1
7	Stainless Steel	200	0.125
8	Stainless Steel	250	0.1
9	Stainless Steel	400	0.22

Table 2 Liquid Properties

Liquid	Density (kg/m^3)	Viscosity (mPa s)	Surface Tension (N/m)
Water	996	1	0.073
Acetone	793	0.30-0.543	0.023
Dodecane	749	1.34	0.025

In order to process the video obtained from the experiments and determine the value of Impact velocity, droplet diameter and spreading ratio, a Matlab code was used.

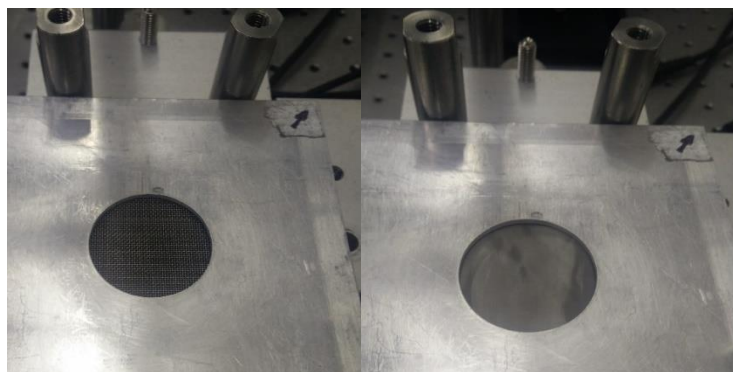


Figure 4 Examples of meshes used for the experiment (samples number 9 & 1).

Considering the different parameters, and principally in the case of water and acetone, the experiments were organised by the following schema in order to analyse all the possible combination of variables.

Table 3 Meshes Properties

Test Group N°	Liquid	Height of Release (cm)	Needle Gauge	Samples used for the impact
1	Water	20.3	21	1-2-4-6-7-8-9
2	Water	44.3	26s	1-2-3-4-5-7
3	Water	80.3	21	1-2-4-6-7-8-9
4	Water	20.3	26s	1-2-3-4-5-7
5	Water	44.3	21	1-2-4-6-7-8-9
6	Water	80.3	26s	1-2-3-4-5-7
7	Acetone	20.3	21	1-2-4-6-7-8-9
8	Acetone	44.3	26s	1-2-3-4-5-7
9	Acetone	80.3	21	1-2-4-6-7-8-9
10	Acetone	20.3	26s	1-2-3-4-5-7
11	Acetone	44.3	21	1-2-4-6-7-8-9
12	Acetone	80.3	26s	1-2-3-4-5-7

The impact was tested using different surfaces in the case of the smallest needle in order to maintain a similar value of the ratio given by $\beta = \frac{D_{pore}}{d}$. The error analysis is reported in the tables below:

Table 4 Impact Velocity Error Analysis Water & Acetone

Height of Release	Needle Gauge	Liquid	Mean Velocity (m/s)	Standard Deviation	Maximum Value (m/s)	Minimum Value (m/s)
20.3	21	Water	1.8	0.18	2.3	1.6
44.3	21	Water	2.7	0.22	3.1	2.2
80.3	21	Water	3.8	0.23	4.2	3.4
20.3	26s	Water	1.8	0.18	2.2	1.4
44.3	26s	Water	2.7	0.21	3.1	2.4
80.3	26s	Water	3.9	0.24	4.4	3.5
20.3	21	Acetone	2.0	0.26	2.5	1.5
44.3	21	Acetone	2.9	0.39	3.8	2.2
80.3	21	Acetone	3.9	0.54	4.8	3.1
20.3	26s	Acetone	1.9	0.20	2.4	1.6
44.3	26s	Acetone	2.9	0.32	3.4	2.3
80.3	26s	Acetone	3.9	0.28	4.5	3.5

Table 5 Initial Diameter Error Analysis Water & Acetone

Needle Gauge	Liquid	Mean Diameter (mm)	Standard Deviation	Maximum Value (mm)	Minimum Value (mm)
21	Water	3.0	0.19	3.5	2.6
26 s	Water	1.9	0.09	2.1	1.6
21	Acetone	1.9	0.12	2.2	1.7
26 s	Acetone	1.7	0.09	2.0	1.5

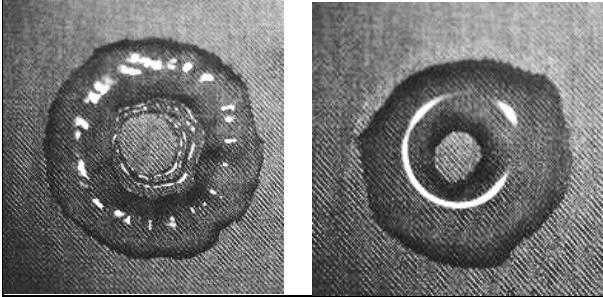
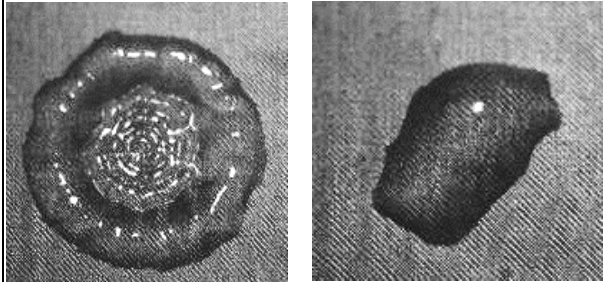
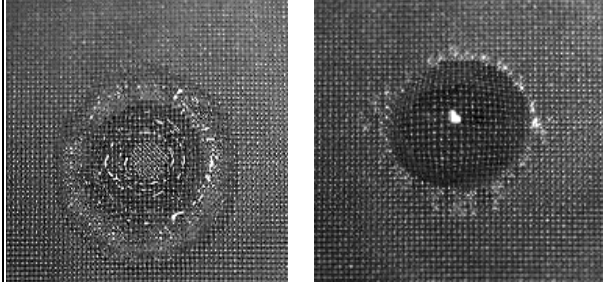
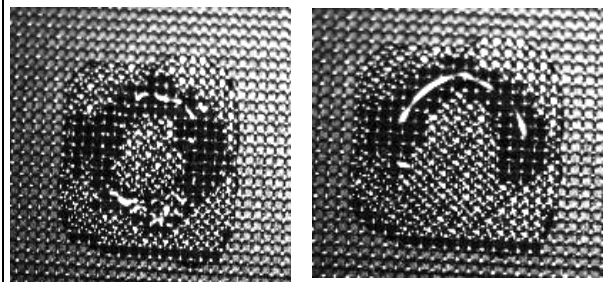
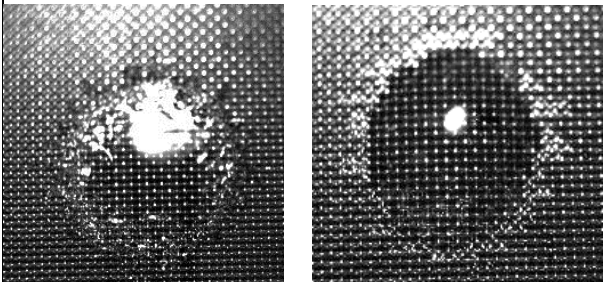
Table 6 Spreading Diameter Error Analysis Water & Acetone

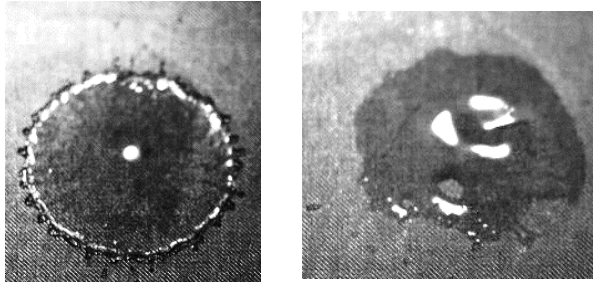
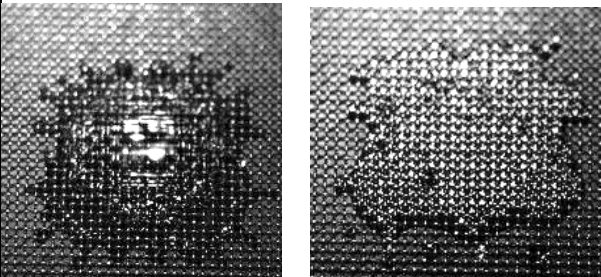
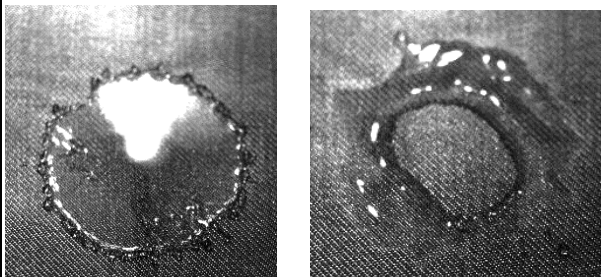
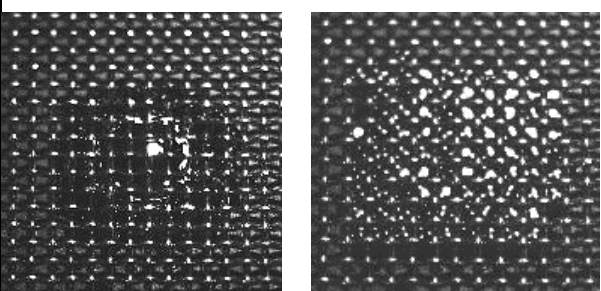
Height of Release	Sample Number	Needle Gauge	Liquid	Mean Spreading (mm)	Standard Deviation	Maximum Value (mm)	Minimum Value (mm)
20.3	1	21	Water	9.6	0.18	9.7	9.100
20.3	4	21	Water	6.5	0.34	7.2	6.1
20.3	7	21	Water	7.4	0.39	7.8	6.9
44.3	1	21	Water	10.7	0.47	11.7	9.9
44.3	4	21	Water	8.6	0.72	10.0	7.8
44.3	7	21	Water	8.1	0.34	8.7	7.9
80.3	1	21	Water	11.9	0.45	12.3	11.0
80.3	4	21	Water	9.4	0.76	10.5	8.5
80.3	7	21	Water	7.8	0.28	8.2	7.4
20.3	1	26s	Water	5.8	0.24	6.1	5.4
20.3	4	26s	Water	4.7	0.29	5.1	4.3
20.3	7	26s	Water	4.6	0.28	5.0	4.1
44.3	1	26s	Water	6.8	0.39	7.4	6.2
44.3	4	26s	Water	5.4	0.67	6.3	4.2
44.3	7	26s	Water	4.4	0.22	4.7	4.1
80.3	1	26s	Water	7.7	0.65	8.5	6.3
80.3	4	26s	Water	4.9	0.45	5.5	4.4
80.3	7	26s	Water	4.7	0.21	4.9	4.6
20.3	1	21	Acetone	7.5	0.22	7.9	7.3
20.3	4	21	Acetone	4.9	0.71	5.9	4.4
20.3	7	21	Acetone	5.7	0.24	6.0	5.4
44.3	1	21	Acetone	9.3	0.45	9.8	8.9
44.3	4	21	Acetone	6.5	0.75	7.4	6.0
44.3	7	21	Acetone	8.8	0.69	9.2	8.0
80.3	1	21	Acetone	6.2	0.30	6.5	5.9
80.3	4	21	Acetone	7.2	0.22	7.5	6.9
80.3	7	21	Acetone	6.9	0.30	7.3	6.7
20.3	1	26s	Acetone	4.5	0.43	5.7	4.5
20.3	4	26s	Acetone	3.9	0.22	4.1	3.9
20.3	7	26s	Acetone	4.3	0.37	5.0	4.3
44.3	1	26s	Acetone	4.5	0.31	5.3	4.5
44.3	4	26s	Acetone	4.5	0.54	5.3	4.5
44.3	7	26s	Acetone	4.3	0.15	4.5	4.3
80.3	1	26s	Acetone	5.5	0.56	5.3	4.0
80.3	4	26s	Acetone	4.1	0.79	6.2	4.8
80.3	7	26s	Acetone	5.1	0.56	5.8	4.4

Results and discussion

In this section, the results obtain by the experiments will be analysed. First of all, it is important to define the regime of different outcomes obtained in the experiment by changing droplet impact velocity and droplet size. The complex outcomes are shown in the following table.

Table 7 Regime Definition

1)		<p>Central imbibition</p> <p>The droplet impacts on the substrate and after the spreading, the recoiling phase is characterised by the formation of a “crater” in the centre of the droplet due to a partial imbibition of the liquid inside the substrate.</p> <p>$d = 3,065 \text{ mm}, v_i = 1,712 \frac{m}{s}, D_{pore} = 25 \mu m, \text{Water}$</p>
2)		<p>Deposition</p> <p>The drop impacts on the substrate, after the spreading and the recoiling it is not possible to observe a proper imbibition and the droplet recoils in an asymmetrical shape.</p> <p>$d = 3,057 \text{ mm}, v_i = 1,7335 \frac{m}{s}, D_{pore} = 25 \mu m, \text{Water}$</p>
3)		<p>Initial imbibition and Deposition</p> <p>The drop impacts on the substrate. Even if after the spreading it is possible to see an initial imbibition, successively the droplet recoils in a symmetric shape and deposition occurs, with a imbibition at the edge of the spread lamella</p> <p>$d = 3,056 \text{ mm}, v_i = 2,179 \frac{m}{s}, D_{pore} = 100 \mu m, \text{Water}$</p>
4)		<p>Partial Imbibition and Deposition</p> <p>The drop impact on the substrate and during the recoiling a partial imbibition occurs. It is possible to observe that part of the liquid is deposited on the substrate.</p> <p>$d = 3,2627 \text{ mm}, v_i = 1,8595 \frac{m}{s}, D_{pore} = 250 \mu m, \text{Water}$</p>
5)		<p>Splash and Deposition</p> <p>The drop impact on the substrate and a splash occurs, in fact, it is possible to see smaller droplets detaching from the central one. Even for higher velocities and larger pores, it is possible to have a deposition instead of an imbibition.</p> <p>$d = 2,8275 \text{ mm}, v_i = 3,065 \frac{m}{s}, D_{pore} = 200 \mu m, \text{Water}$</p>

<p>6)</p> 	<p>Splash and Partial Imbibition</p> <p>The drop impacts on the substrate and a splash occurs, even if the main effect is given by deposition it is possible to observe a partial imbibition</p> <p>$d = 3,552 \text{ mm}, v_i = 2,6619 \text{ m/s}, D_{pore} = 25\mu\text{m}, \text{Water}$</p>
<p>7)</p> 	<p>Splash and Total Imbibition</p> <p>The drop impacts on the substrate and after the splash a total imbibition occurs. It was observed that this kind of outcome is more common for surfaces with larger pores.</p> <p>$d = 2,8595 \text{ mm}, v_i = 2.9098 \frac{\text{m}}{\text{s}}, D_{pore} = 250 \mu\text{m}, \text{Water}$</p>
<p>8)</p> 	<p>Splash and Central Imbibition</p> <p>The drop impact on the substrate and a splash occurs. Finally in this case it is possible to observe a central imbibition.</p> <p>$d = 1,93 \text{ mm}, v_i = 2,527 \frac{\text{m}}{\text{s}}, D_{pore} = 100 \mu\text{m}, \text{Water}$</p>
<p>9)</p> 	<p>Total imbibition</p> <p>The drop impact on the substrate and a total imbibition occurs. This outcome was mainly observed in the case of substrate 9, with pores dimension of $400 \mu\text{m}$.</p> <p>$d = 3,234 \text{ mm}, v_i = 1,958 \frac{\text{m}}{\text{s}}, D_{pore} = 400 \mu\text{m}, \text{Water}$</p>

In the case of the sample number 9 ($D_{pore} = 400 \mu\text{m}$) it was not possible to identify a proper spreading because, due to the larger dimension of the pores, the imbibition was really quick despite the lower value of impact velocity. On the other hand, the outcome given by deposition is more common in the case of impact on substrate with pores of smaller dimension like substrate 1,3 and 4 and for lower impact velocities. Results show that deposition occurs mainly for the first and fourth test group of experiments, except in the case of surfaces 8 and 9 in which total imbibition occurs. In the case of test group 2 and 5 it was extremely difficult to observe a deposition outcome and the impact was mainly characterised by central or partial imbibition, with splash in a few cases. In the case of test group 3 and 6 a splash outcome was observed with central total or partial imbibition.

In the following graph is shown the distribution of the different regimes in the case of Water, in function of We number and the ratio of dynamic (p_d) and capillary (p_c) pressures. It is possible to observe that deposition occurs in the case of low Weber Number, and the total imbibition mainly in the region in which the ratio between the pressure is lower and in which the impact velocity and pores size are growing.

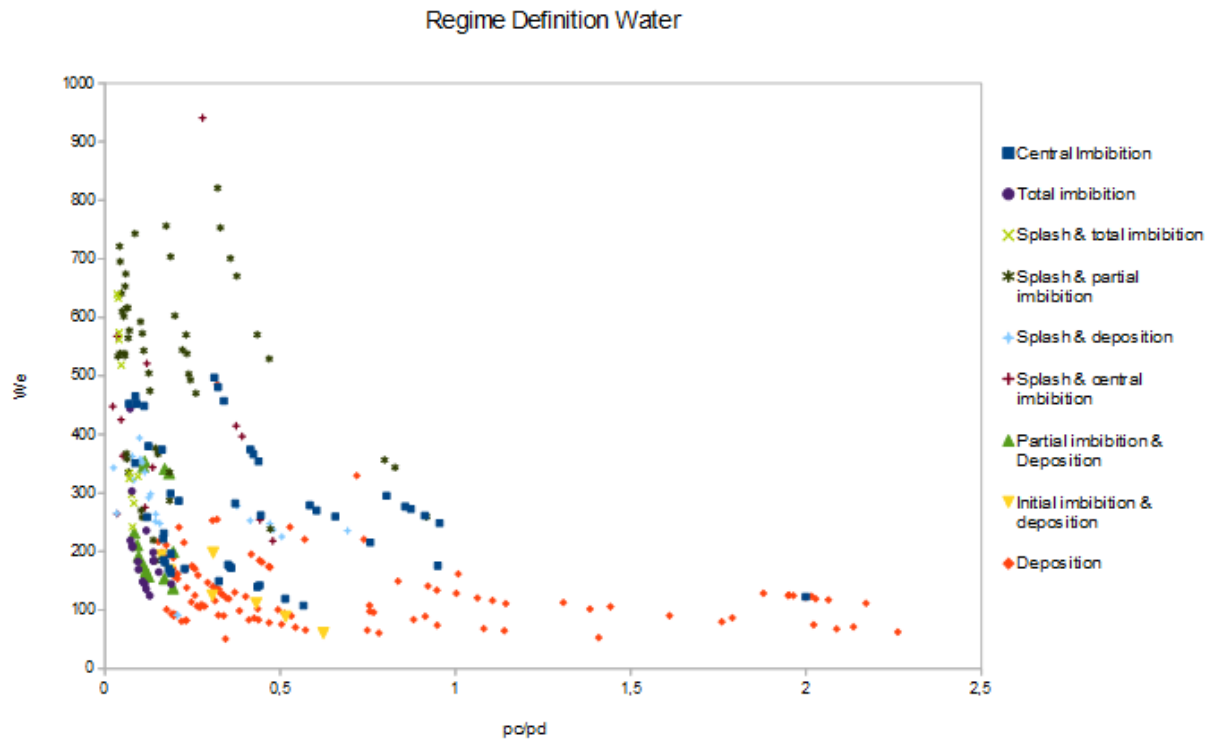


Figure 5 Regime distribution for water considering all the experimental data between case 1 and case 6, in function of pressure ratio.

An attempt to compare the results with a similar graph obtained by defining the distribution of the regimes in function of We number and the value given by was made $1/\beta$. Again, the deposition outcome is mainly centred in the area with lower Weber Number and $1/\beta$, that corresponds to a lower velocity of impact and to a smaller pore dimension, by increasing pore dimension and velocity partial imbibition and total imbibition occurs but it showed that the total imbibition is mainly influenced by pore size.

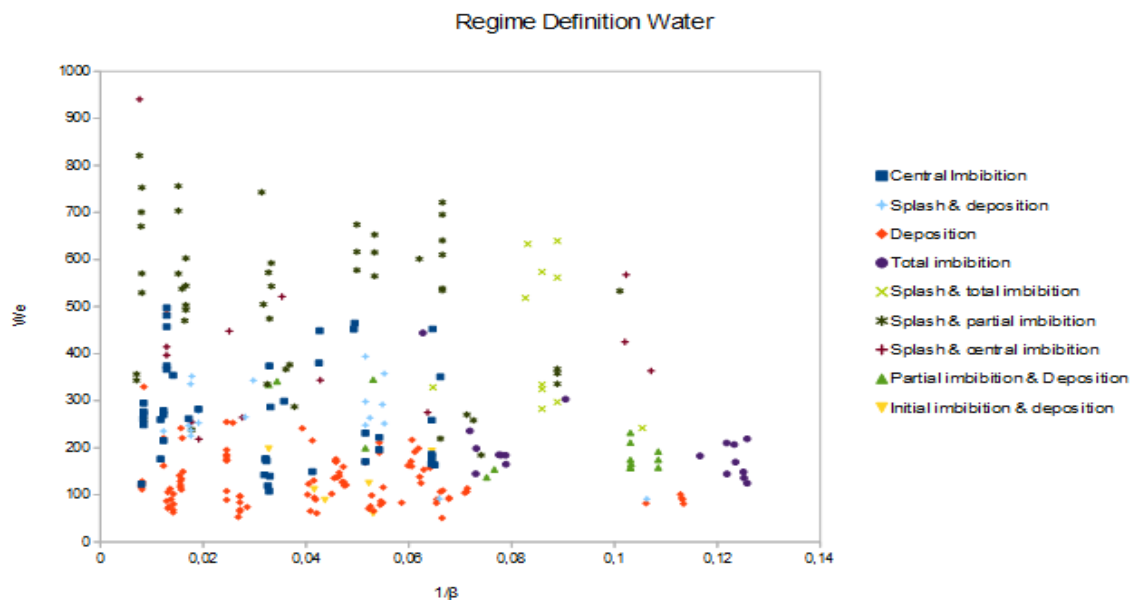


Figure 6 Regime distribution for water considering all the experimental data between case 1 and case 6, in function of $\frac{1}{\beta}$

In comparing the regime map for impacts obtained by using different needles, it is possible to observe that, considering the same value of β , a distribution outcome is more common in the case of droplet with a smaller diameter and that the findings are mainly consistent with a lower value of the Weber Number.

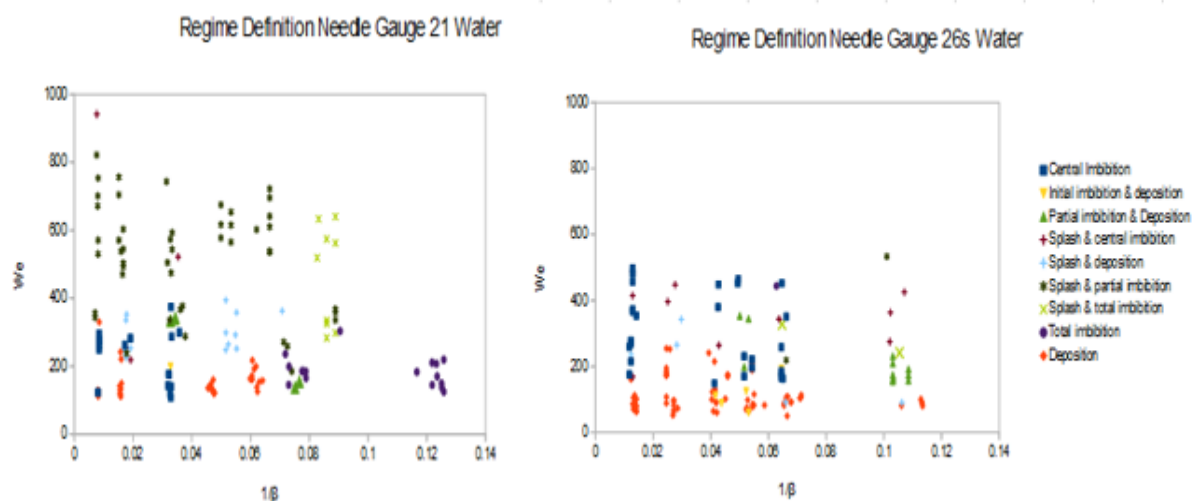


Figure 7 Regime distribution for water considering the results obtained by using two different needle size

The same graphs are reported in the case of Acetone. The identified regimes are the same already observed in the case of water.

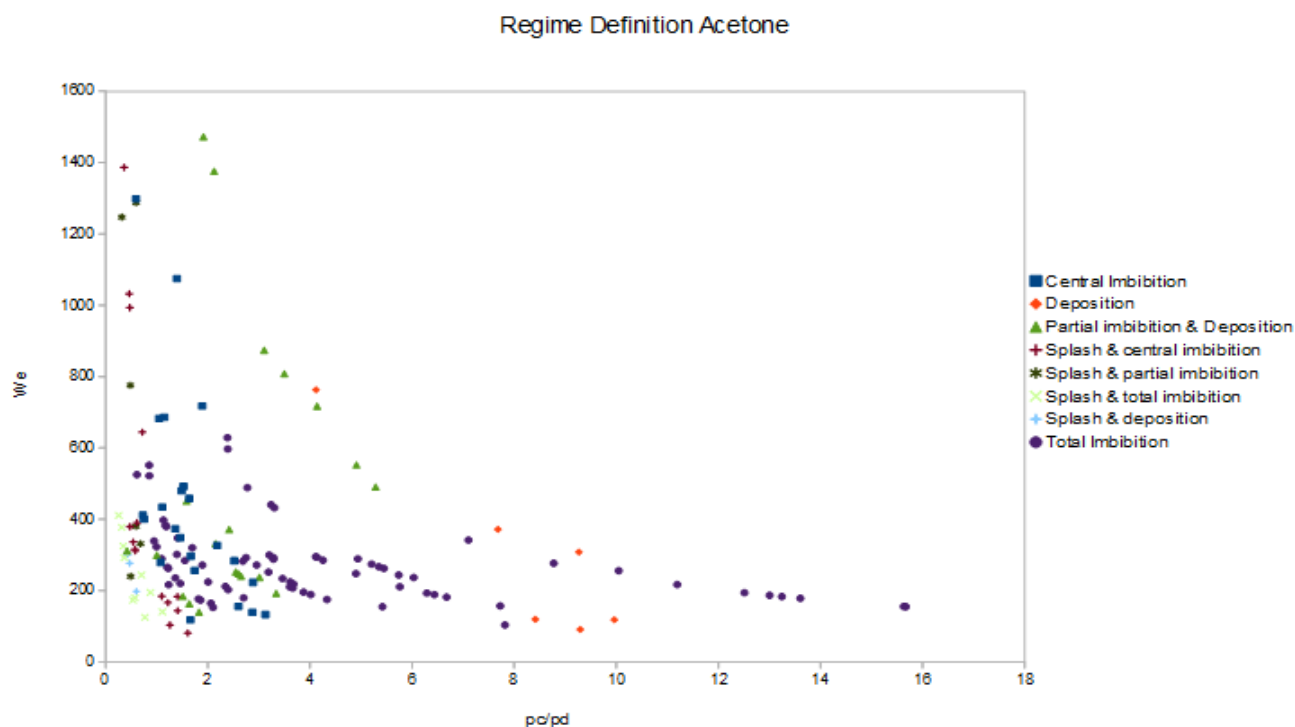


Figure 8 Regime distribution for acetone considering all the experimental data between case 7 and case 12, in function of pressure ratio.

Due to the lowest surface tension of the acetone, the outcome characterised by total imbibition is more common compared to the results obtained with water.

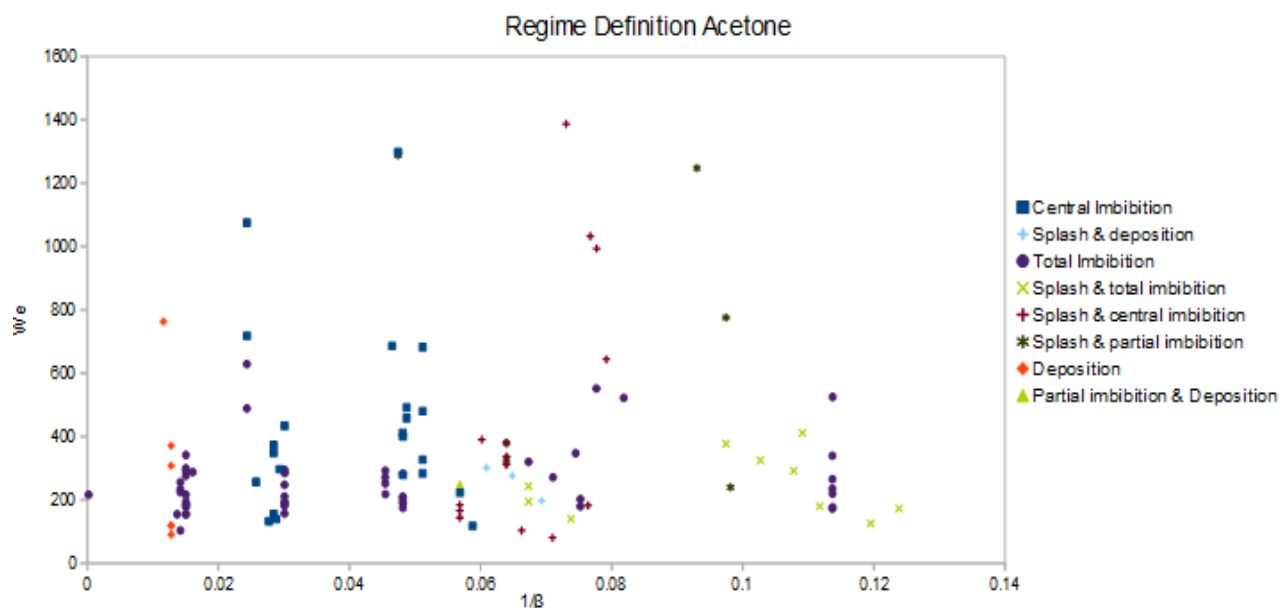


Figure 9 Regime distribution for acetone considering all the experimental data between case 7 and case 12, in function of $\frac{1}{\beta}$.

Again it is shown that total imbibition is mainly influenced by pore size and that by increasing velocity, other outcomes characterised by an incomplete imbibition, central or partial, occurs. In the case of acetone, the outcome defined as “initial imbibition & deposition” was not observed.

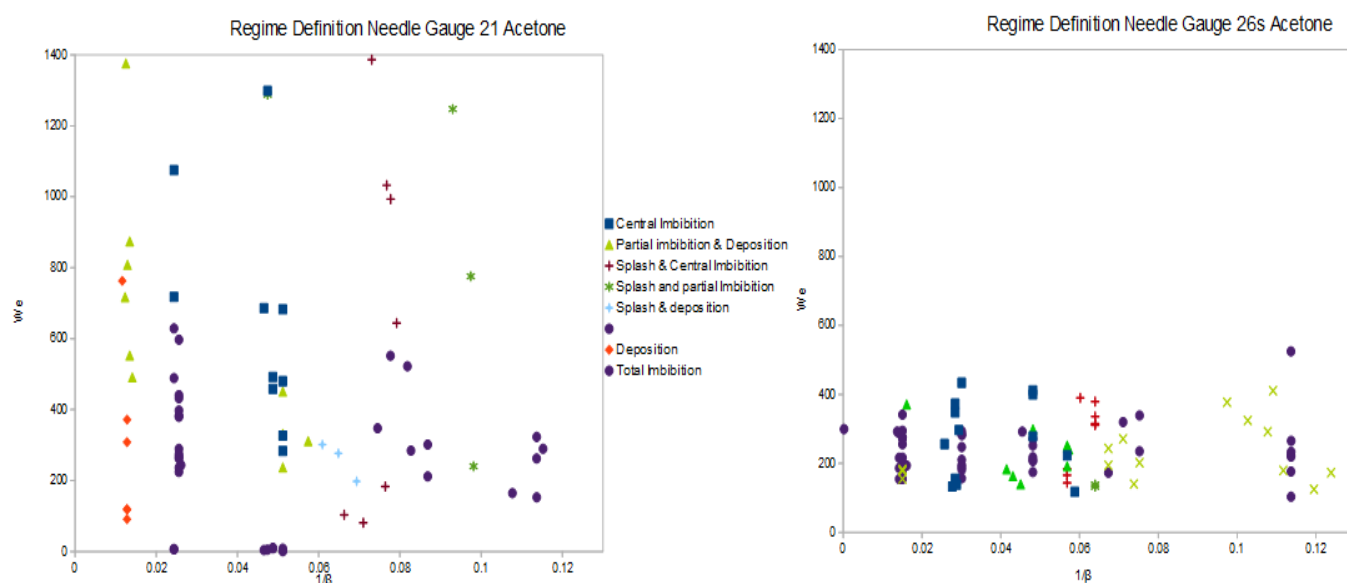


Figure 10 Regime distribution for acetone considering the results obtained by using two different needle size

It is possible to observe that, considering the same value of β , the distribution of different regimes is similar in both cases but it is not possible to define a deposition for the experiments referred to impact of droplets with smaller diameter. In the last graph the distribution of data gained for both liquids, water and acetone, is reported in function of Weber and Reynolds number.

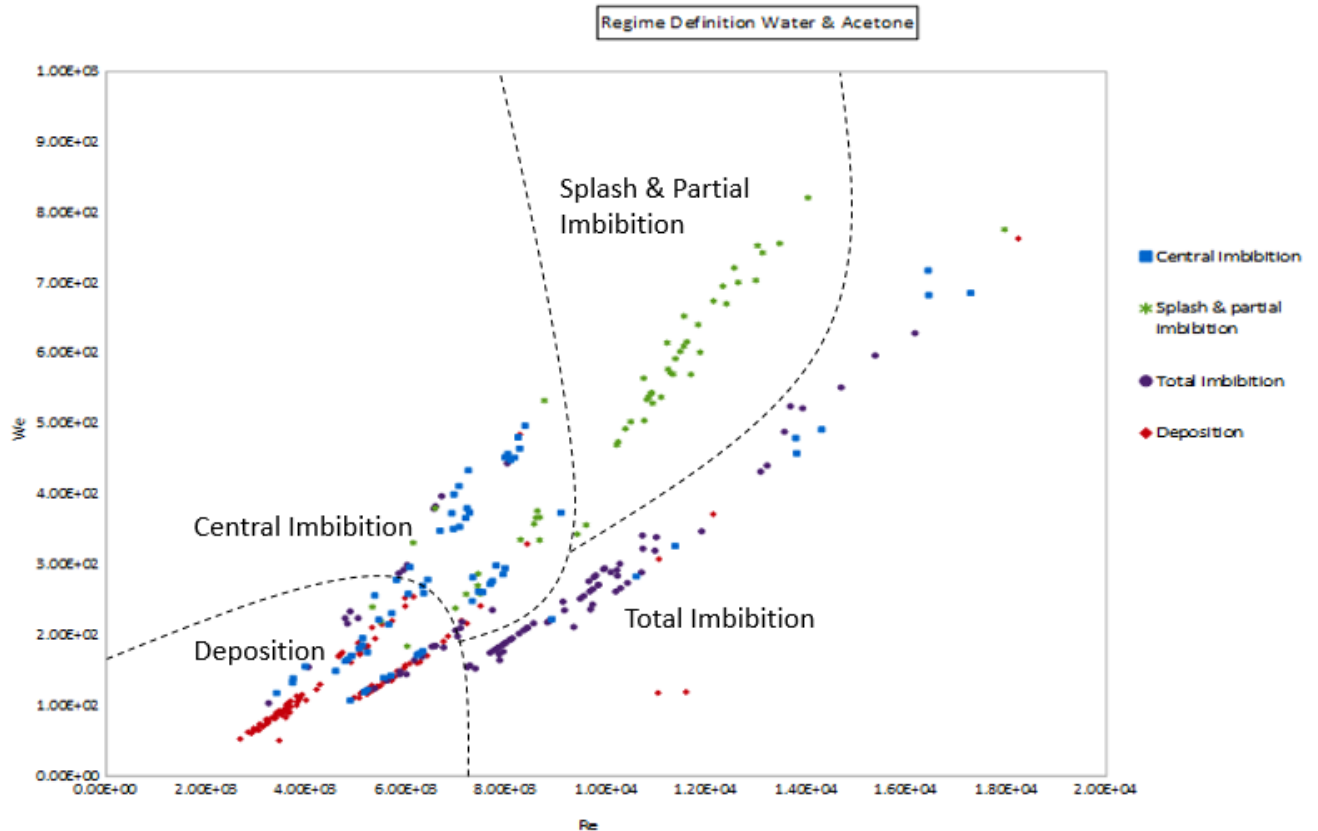


Figure 11 Regime distribution for all the experimental data in function of Weber and Reynolds number.

By observing the Figure 11 it is possible to distinguish four dominant outcomes that are: deposition, in a range of Reynolds number between 3000-5000 and a Range of Weber number between 50-150, that corresponds to a lower impact velocity, central imbibition, in a range of Reynolds number between 5000-7000 and a range of Weber number between 100-500. By increasing Reynolds number but approximately in the same range of Weber number, the more common outcome given is the total imbibition whereas by increasing velocity, so in a range of Reynolds number between 11000-15000 and a range of Weber number between 500-1000, splash with partial imbibition occurs.

Conclusion

This preliminary study is focused on the investigation of droplet impact on porous surfaces with a wide range of pore size. It was found that a total imbibition occurs mainly in the case of meshes with pores of larger size, whereas the influence of a higher impact velocity and consequently a higher Weber number, brings to a splash outcome and to a partial imbibition. By comparing the data obtained for water and acetone it was found that a total imbibition is also influenced by viscosity and surface tension. The total imbibition is almost instantaneous in the case of impact of acetone droplets on surface with a pore size in a range between 200-400 μm that brings difficulties in defining a proper spreading diameter. Finally, the experiments show that for the same value of β but for a different combination of pore size and droplet initial diameter (even if in the case of acetone the difference is very small), a similar regime distribution is observed.

Acknowledgements

I would like to acknowledge the support of Quentin Lelievre, internship student from the Université Toulouse Paul Sabatier

Nomenclature

p_d	Dynamic pressure [Pa]
p_c	Capillary pressure [Pa]
σ	Surface tension [N/m]
ρ	Liquid density [kg/m^3]
D_{pore}	Pore diameter [m]
d	Droplet diameter [m]

v_i	Impact velocity [m s^{-1}]
We	Weber number
Re	Reynolds number

References

- [1] Volfango Bertola (2008), Some applications of controlled drop deposition on solid surfaces, *Recent Patents on Mechanical Engineering*, 167-164.
- [2] Woo Shik Kim, Sang Yong Lee, (2014). Behavior of a water drop impinging porous substrates-examination of contact-line drag effect, *Atomizations and Sprays*, 257-274.
- [3] Mirosław Weclas (2010), Potential of Porous-Media Combustion Technology and Applied to Internal Combustion Engines, *Journal of Thermodynamics*, Article ID 789262 and, p. 31-45.
- [4] Marco Marengo, Carlo Antonini, Ilia V. Roisman, Cameron Tropea (2011). *Drop collisions with simple and complex surfaces*, *Current Opinion in Colloid & Interface Science* 16, pp. 292-302.
- [5] Ilia V. Roisman, A. L. (2015). Drop splashing induced by target roughness and porosity: The size plays no role. *Adv Colloid Interface Sci.*, p. 615-621.
- [6] Neyval C. Reis Jr, Richard F. Griffiths, Jane Méri Santos (2007), Parametric study of liquid droplets impinging on porous surfaces, *Applied Mathematical Modelling* 32, 341-361
- [7] R.P. Sahu, S. S. (2015). Impact of aqueous suspension drops onto non-wettable porous membranes: Hydrodynamic focusing and penetration of nanoparticles. *Colloids and Surfaces A: Physicochemical*
- [8] Zouhaier Romdhani, Ayda Baffoun, Mohamed Hamdaoui, Sadok Roudesli (2014). Drop Impact on Textile Material: Effect of Fabric Properties, *Autex Research Journal*, Vol. 14, No 3.
- [9] Woo Shik Kim, Sang Yong Lee, (2014). Behavior of a water drop impinging on heated porous surfaces, *Experimental Thermal and Fluid Science* 55, 62-70.
- [10] Yarin, A. (2006, January). DROP IMPACT DYNAMICS: Splashing, Spreading, Receding, Bouncing. *Annual Review of Fluid Mechanics*, 38, p. 159-192.
- [11] Sathish M. Kumar, A. P. (2006). Dynamic of drop spreading on fibrous porous media. *Colloid and Surfaces A*, pp. 157-163.